

SUPPORTING INFORMATION

Polynuclear Tantalum(V) Coordination Complexes. From dinuclear $\{\text{Ta}_2\text{O}\}$ to octanuclear $\{\text{Ta}_8\text{O}_{12}\}$ oxo species connected through aryl monotopic carboxylate linkers

Alejandro Vieyra Huerta,^a Mahmud Beji Ahmed,^b Nadine Essayem,^b Laurent Djakovitch,^b Adel Mesbah,^b Thierry Loiseau^a and Sylvain Duval^{a,*}

Contribution from

^aUnité de Catalyse et Chimie du Solide (UCCS) – UMR CNRS 8181, Université de Lille, Centrale Lille, Université d'Artois, F-59000 Lille, France.

* To whom correspondence should be addressed. E-mail: sylvain.duval@univ-lille.fr, Phone: (33) 3 20 43 40 13, Fax: (33) 3 20 43 48 95.

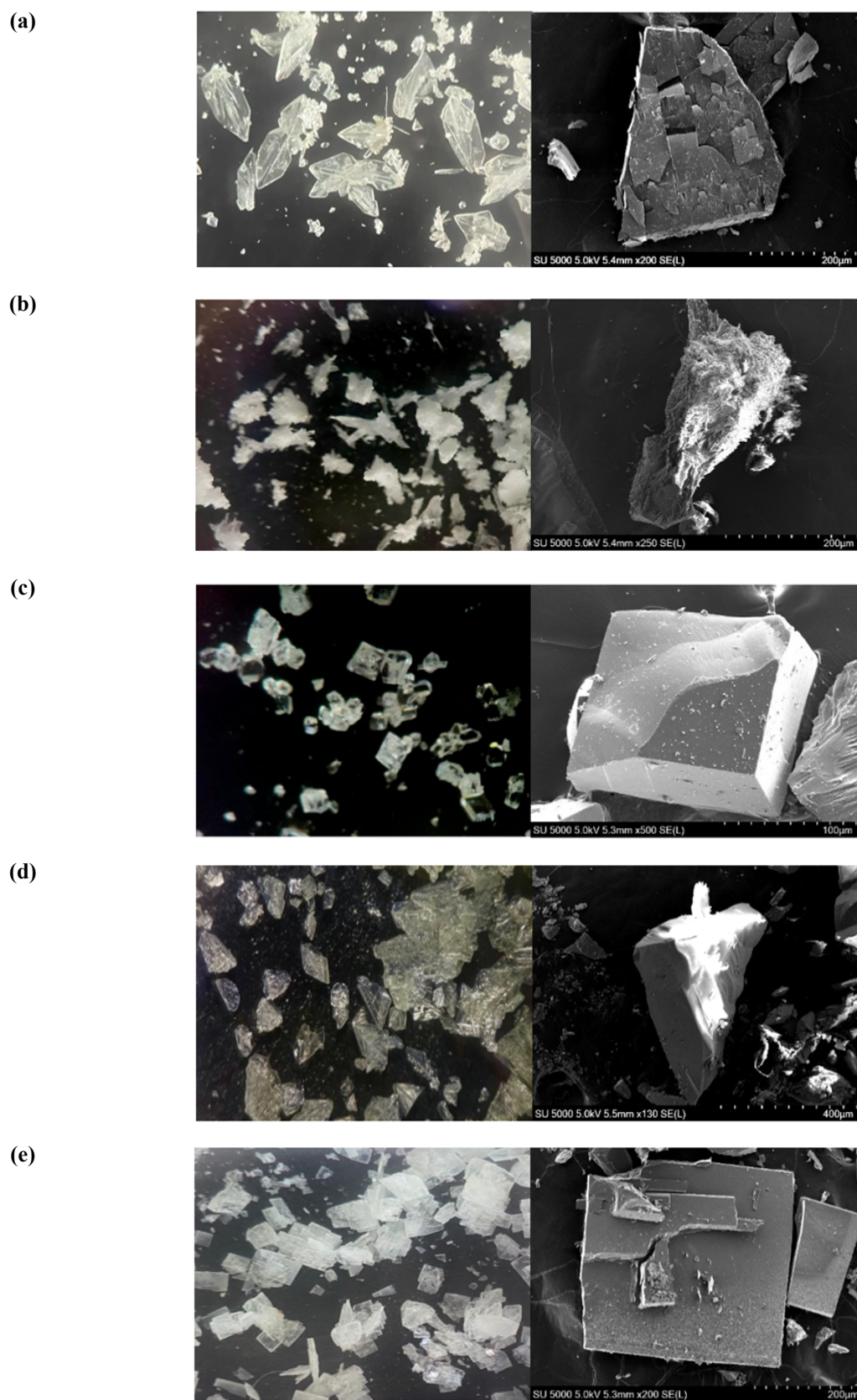


Figure S1. Optical microscope and SEM photographs of crystals of complexes **1(a)**, **2(b)**, **3(c)**, **4(d)** and **5(e)**

Powder XRD patterns

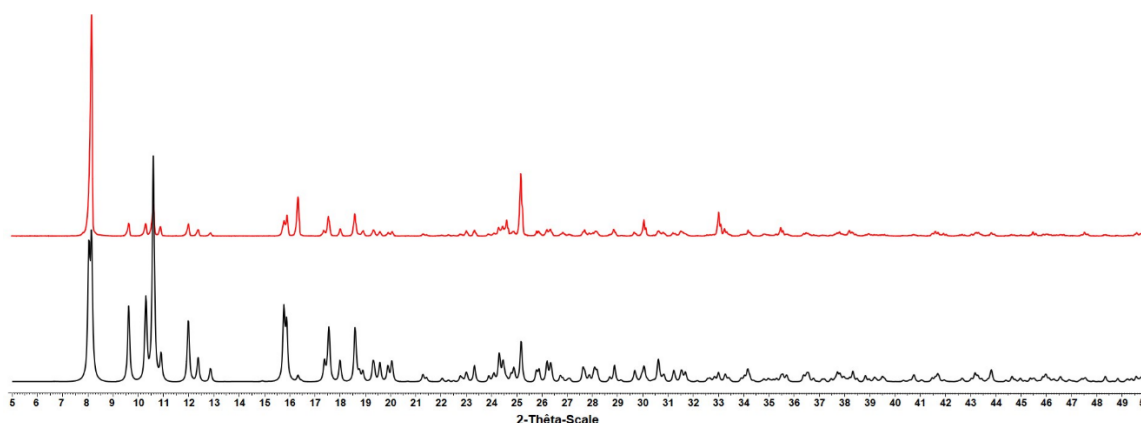


Figure S2a. Comparison of the experimental powder XRD pattern (red line) of complex 1 with the calculated one (black line). X-ray source; Copper $K\alpha$ radiation.

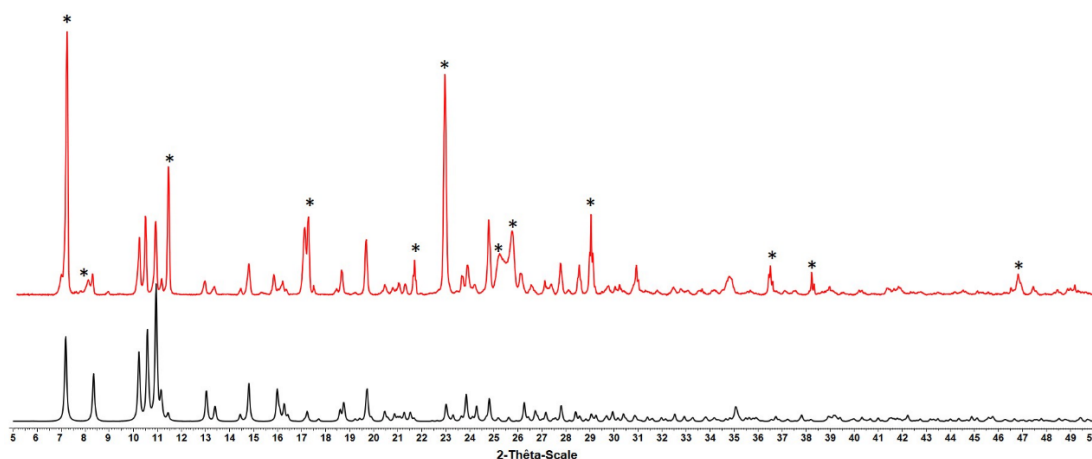


Figure S2b. Comparison of the experimental powder XRD pattern (red line) of complex 2 with the calculated one (black line). X-ray source; Copper $K\alpha$ radiation. The (*) represent unidentified crystalline impurities within the sample.

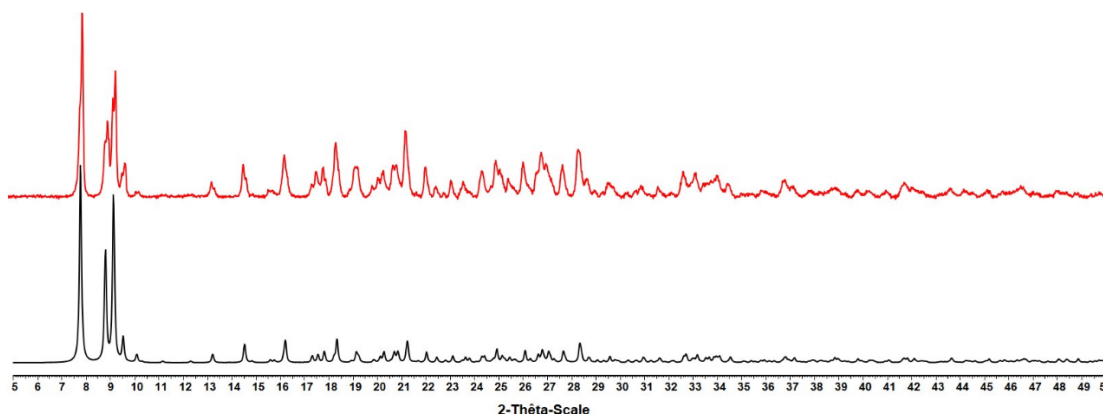


Figure S2c. Comparison of the experimental powder XRD pattern (red line) of complex 3 with the calculated one (black line). X-ray source; Copper $K\alpha$ radiation.

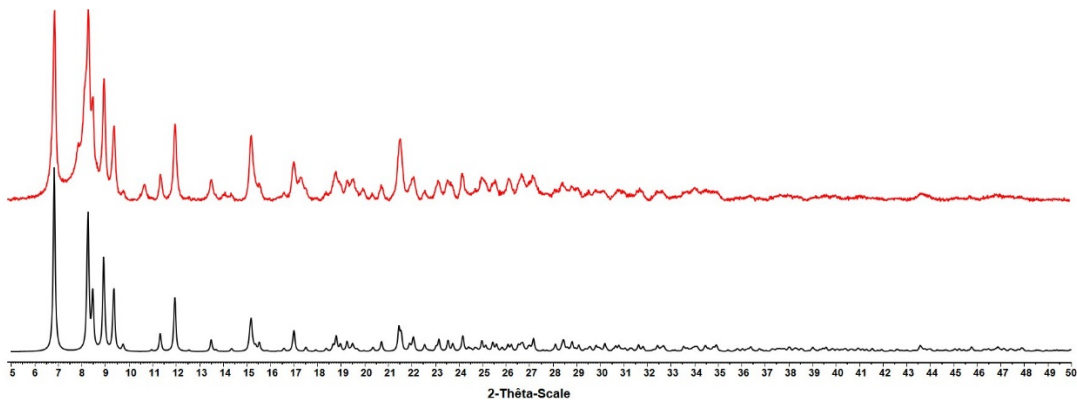


Figure S2d. Comparison of the experimental powder XRD pattern (red line) of complex **4** with the calculated one (black line). X-ray source; Copper $K\alpha$ radiation.

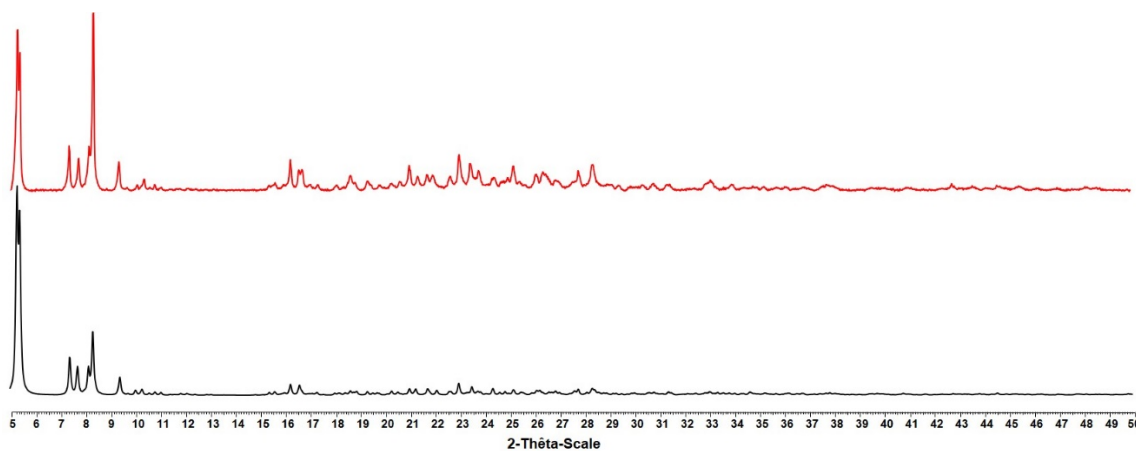


Figure S2e. Comparison of the experimental powder XRD pattern (red line) of complex **5** with the calculated one (black line). X-ray source; Copper $K\alpha$ radiation.

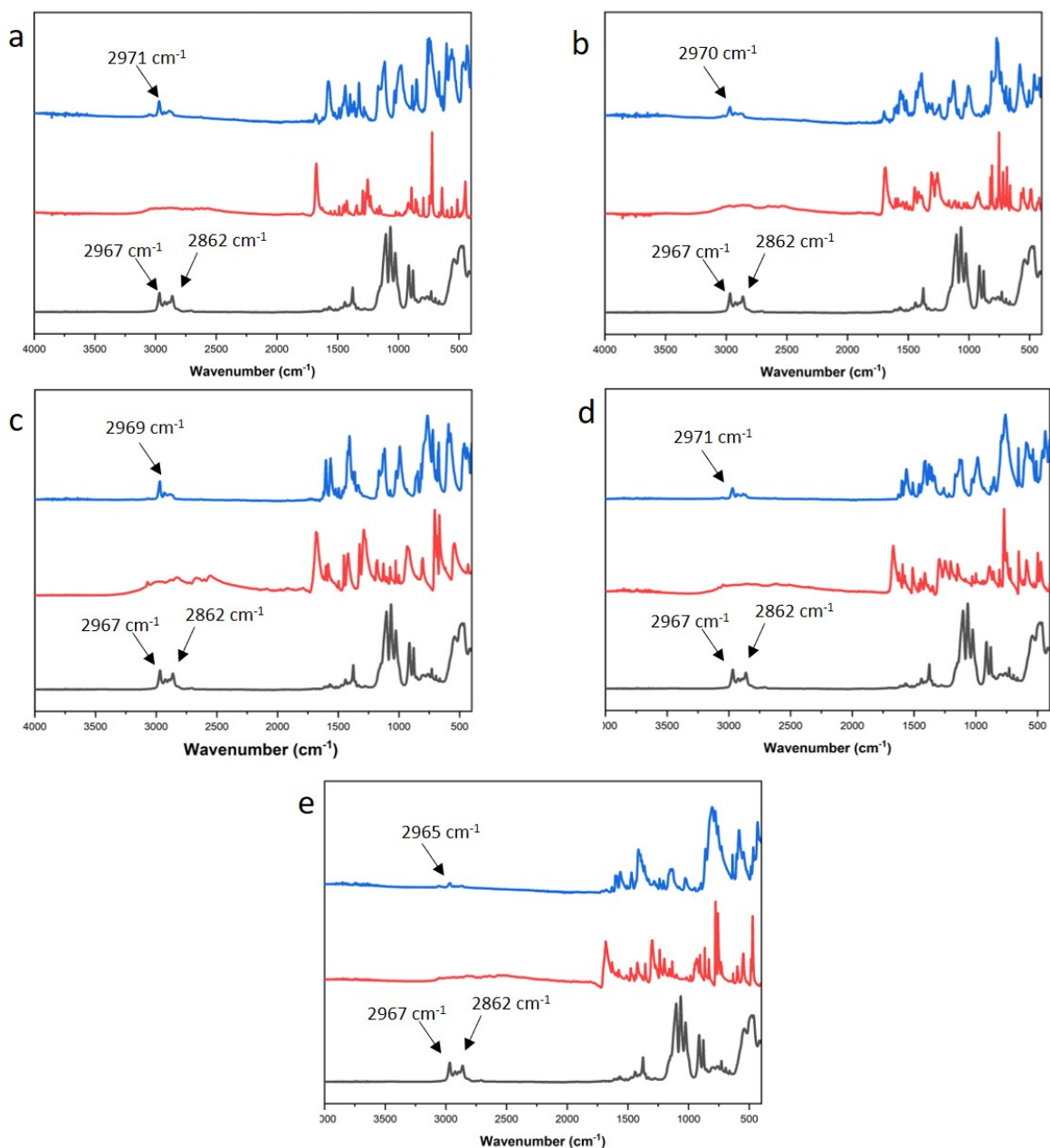


Figure S3a. Infrared spectroscopy analysis in the 4000 – 400 cm^{-1} range for the tantalum complexes **1** (a), **2** (b), **3** (c), **4** (d), **5** (e) (blue lines). The free ligands anthracene-9-carboxylic acid (a), 4'-methylbiphenyl-4-carboxylic acid (b), benzoic acid (c), 1-naphtoic acid (d) and 2-naphtoic acid (e) (red lines) and the tantalum precursor $\text{Ta}(\text{OEt})_5$ (black lines).

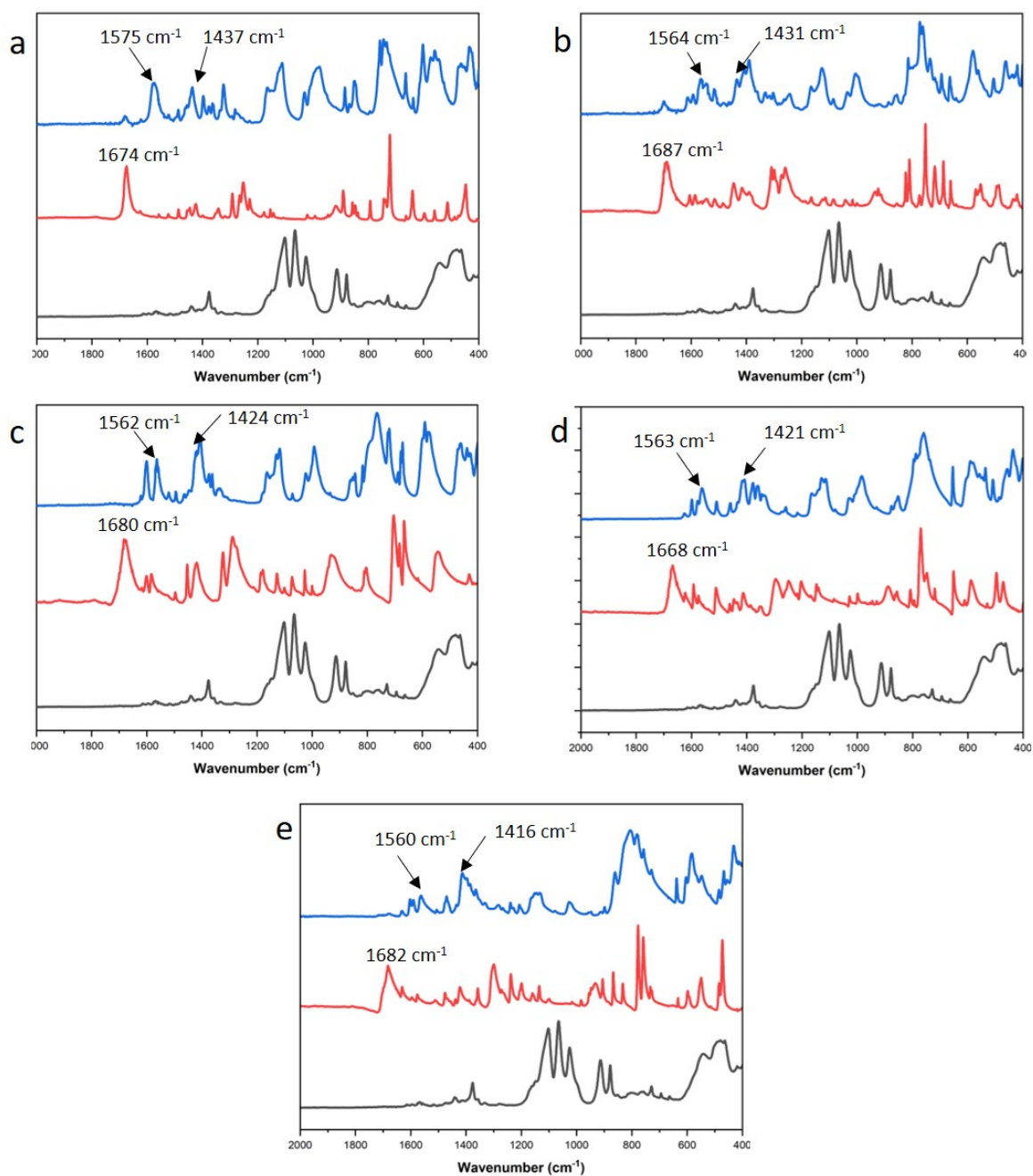


Figure S3b. Infrared spectroscopy analysis in the 2000 – 400 cm^{-1} range for the tantalum complexes **1** (a), **2** (b), **3** (c), **4** (d), **5** (e) (blue lines). The free ligands anthracene-9-carboxylic acid (a), 4'-methylbiphenyl-4-carboxylic acid (b), benzoic acid (c), 1-naphtic acid (d) and 2-naphtic acid (e) (red lines) and the tantalum precursor $\text{Ta}(\text{OEt})_5$ (black lines).

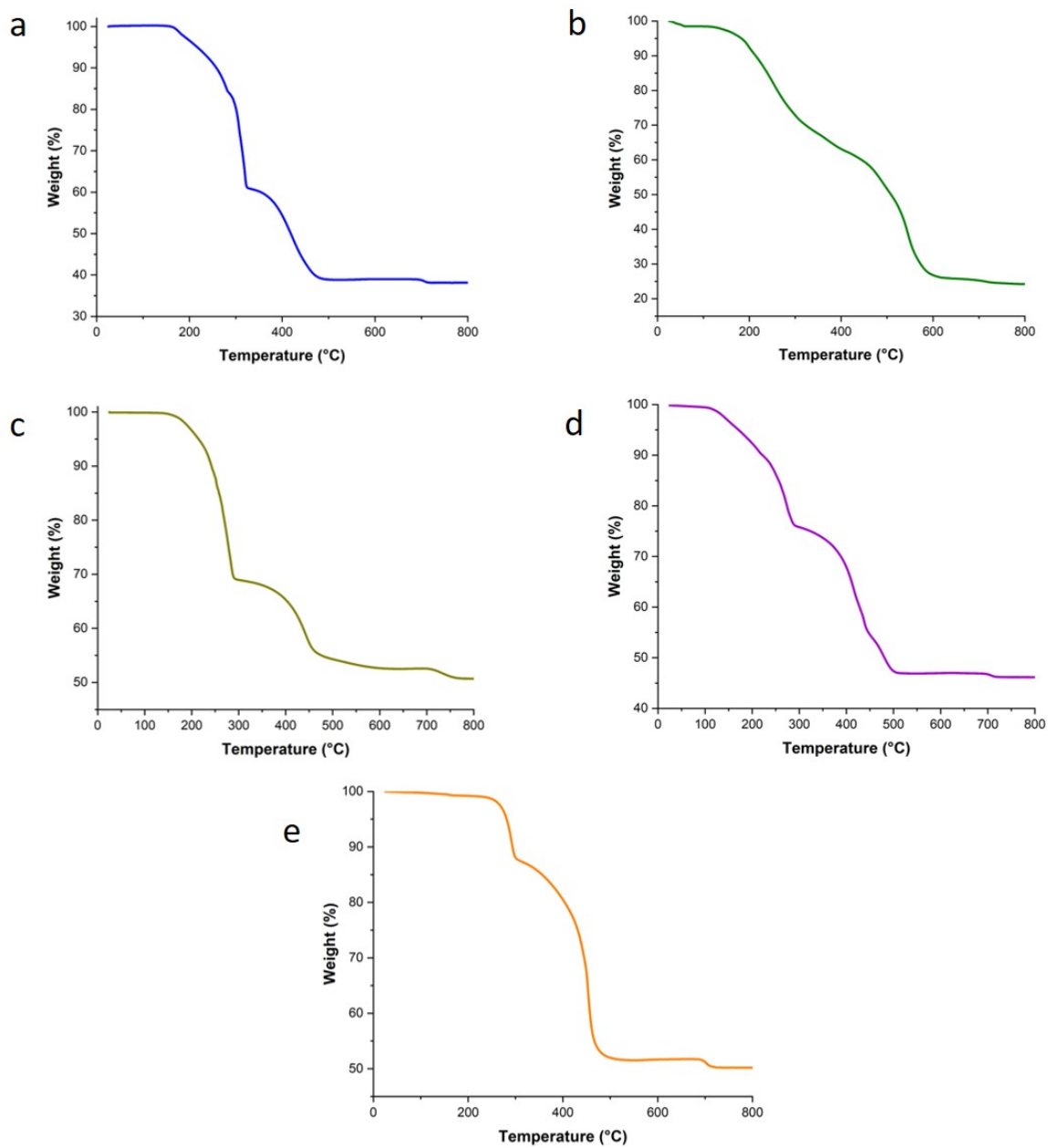


Figure S4. TGA of the tantalum complexes **1** (a), **2** (b), **3** (c), **4** (d), **5** (e).

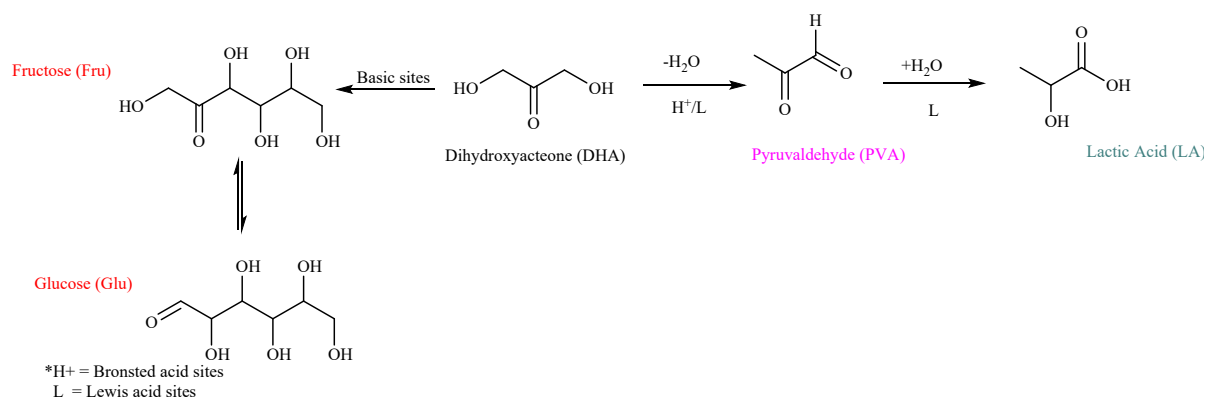


Figure S5. Catalytic reaction scheme of the conversion of dihydroxyacetone (DHA) into lactic acid (LA), pyruvaldehyde (PA) and sugars (C₆, such as glucose or fructose).